

Competitive energy and electron-transfer quenching across the peptide-bridge in polypyridine ruthenium(II)/osmium(II) binuclear systems

M. Furue ^{a,*}, M. Ishibashi ^b, A. Satoh ^b, T. Oguni ^b,
K. Maruyama ^b, K. Sumi ^a, M. Kamachi ^b

^a *Department of Environmental Systems Engineering, Kochi University of Technology, Tosayamada, Kochi 782-8502, Japan*

^b *Department of Macromolecular Science, Graduate School of Science, Osaka University, Toyonaka, Osaka 560-0043, Japan*

Received 23 September 1999; accepted 15 December 1999

Contents

Abstract	104
1. Introduction	104
2. Experimental	105
2.1 Materials	105
2.2 4-(Boc-Leu-NH)-bpy	105
2.3 4-(Boc-Pro-NH)-bpy	106
2.4 4'-{N-[bis(4,4'-bis(trifluoromethyl)-2,2'-bipyridine)(4'-methyl-2,2'-bipyridine-4-carbonyl)-ruthenium(II)-Leu-NH]-bpy dichloride	106
2.5 4'-[(Ru(II)(BTFMB) ₂ mb-4-CO)-Leu-NH]-bpyOs(II)b ₂ (PF ₆) ₄ , I(L = BTFMB) and other binuclear systems I(L = b), II(L = b and BTFMB)	106
2.6 Physical measurements	107
3. Results and discussion	107
References	113

Abbreviations: bpy or b, 2,2'-bipyridine; BTFMB, 4,4'-bis(trifluoromethyl)-2,2'-bipyridine; [b₂Ru(II)mb-4-COOH]Cl₂, bis(2,2'-bipyridine)(4'-methyl-2,2'-bipyridine-4-carboxylic acid)ruthenium(II) dichloride; Boc, *tert*-butoxycarbonyl; DMF, *N,N*-dimethylformamide; EDC, 1-ethyl-3-(3-dimethylaminopropyl)carbodiimide; IBCF, isobutyl chloroformate; Leu, L-leucine; NH₂-bpy, 4-amino-2,2'-bipyridine; THF, tetrahydrofuran.

* Corresponding author. Tel.: +81-887-572516; fax: +81-887-572520.

E-mail address: mfurue@env.kochi-tech.ac.jp (M. Furue).

Abstract

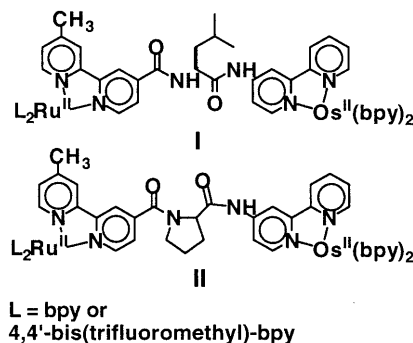
In the excited state of the peptide-bridged Ru(II)/Os(II) binuclear complex, $[L_2Ru(II)-mbCO-L-Leu-NHbpyOs(II)(bpy)_2]$ and $[L_2Ru(II)mbCO-L-Pro-NHbpy-Os(II)(bpy)_2]$ [$L = bpy$ ($= 2,2'$ -bipyridine) or BTFMB ($= 4,4'$ -bis-trifluoromethyl-2,2'-bipyridine), and $mb = 4$ -methyl-bpy], a nearly complete quenching of $Ru^{II} \rightarrow \pi^*$ (Ligand) MLCT emission was observed at room temperature. Lifetime measurements were performed to evaluate the quenching rate and the mechanism on a quantitative basis. In complexes with $L = bpy$, the intramolecular energy transfer process had a unitary efficiency. In complexes with $L = BTFMB$, the evidence for the occurrence of competitive energy and electron-transfer processes was provided from the time dependence of the emission spectra. The main pathway for energy-transfer in both systems could be explained by the Förster mechanism. It was suggested that the direction of MLCT excitation to either bridging or non-bridging bpy-ligand causes the large difference of dipole–dipole distance. © 2000 Elsevier Science S.A. All rights reserved.

Keywords: Electron transfer quenching; Competitive energy; Peptide bridge

1. Introduction

The excited-state properties of polypyridine complexes of d^6 transition-metals such as Ru(II), Os(II), and Re(I) can be tuned by ligands and solvent environment [1]. Recently we have synthesized a new class of bipyridine ligands containing a trifluoromethyl group as a substituent. 4,4'-Bistrifluoromethyl-2,2'-bipyridine (BTFMB) ligand has a lower lying π^* level which not only leads to significant changes in ground- and excited-state redox potentials but also exerts relatively large effects on absorption and emission spectral properties [2,3].

In this paper we report results showing that competitive energy and electron-transfer quenching of excited Ru(II) by Os(II) complex occurs intramolecularly in the peptide-bridged complexes **I** and **II** with BTFMB ligand. The kinetic study by the time-correlated single-photon counting method was performed to evaluate the quenching rate and the mechanism on the quantitative basis. The results have indicated that the energy-transfer process can be interpreted in terms of the Förster mechanism. Complexes **I** and **II** with bpy ligand were also studied in which only the energy-transfer quenching took place. Comparison of the energy-transfer kinetics



has been made in both systems. The difference of rates can be rationalized by the dipole–dipole distance. Namely, the direction of metal-to-ligand charge-transfer (MLCT) excitation to either bridging or non-bridging bpy-ligand causes the large difference of dipole–dipole distance.

2. Experimental

2.1. Materials

The starting materials, 4,4'-dimethyl-2,2'-bipyridine and 2,2'-bipyridine were purchased from Tokyo Kasei and recrystallized from ethanol. Isobutyl chloroformate (IBCF), 1-ethyl-3-(3-dimethylaminopropyl)carbodiimide (EDC), *tert*-butoxycarbonyl-*L*-leucine (Boc-Leu-OH), and *tert*-butoxycarbonyl-*L*-proline (Boc-Pro-OH) were purchased from Wako Chemicals.

Ru(bpy)₂Cl₂ was prepared as described by Sullivan et al [4]. Os(bpy)₂Br₂ was prepared as described by Buckingham et al. [5]. 4-Methyl-2,2'-bipyridine-4'-carbaldehyde was prepared as described previously [6]. 4,4'-Bis(trifluoromethyl)-2,2'-bipyridine (BTFMB) and Ru(BTFMB)₂Cl₂ were synthesized by the same procedure as previously reported by us [2].

4-Methyl-2,2'-bipyridine-4'-carboxylic acid was prepared by the oxidation of the corresponding aldehyde (1.8 g, 9.1 mmol) with Ag₂O (2.3 g, 9.9 mmol) in water (10 ml) with 10% NaOH (5 ml) at room temperature [7] (1.5 g, 77.1%), mp 280°C: ¹H-NMR (DMSO-d₆) δ = 2.44 (s, 3H), 7.30 (m, 1H), 7.85 (dd, 1H), 8.30 (s, 1H), 8.60 (d, 1H), 8.85 (m, 2H); Anal. Calc. for C₁₂H₁₀N₂O₂: C, 67.28; H, 4.71; N, 13.08. Found: C, 67.79; H, 4.67; N, 13.22.

4-Amino-2,2'-bipyridine (4-NH₂-bpy) was prepared by the reduction of 4-nitro-2,2'-bipyridine 1-oxide [8] with sodium borohydride in the presence of 10% palladium-carbon in methanol at room temperature [9].

2.2. 4-(Boc-Leu-NH)-bpy

To a solution of Boc-Leu-OH (675 mg, 2.92 mmol) in dry THF (10 ml) was added triethylamine (293 mg, 2.92 mmol) at room temperature. Then IBCF (396 mg, 2.9 mmol) was added at –15°C. After 15 min, a solution of 4-NH₂-bpy (500 mg, 2.92 mmol) in THF (10 ml) was added dropwise at –15°C. The flask was fitted with an anhydrous CaCl₂ drying tube, and the reaction mixture was stirred overnight at room temperature. After rotary evaporation of THF, the residue was dissolved in ethyl acetate. The solution was washed with aqueous solutions of 10% citric acid and 5% NaHCO₃, and water. Solvent was removed by rotary evaporation and the residue was chromatographed on silica gel with ethyl acetate eluent. The product was obtained as a colorless viscous oil; 230 mg (20.5% yield). ¹H-NMR (CDCl₃) δ = 0.9 (m, 6H), 1.5 (s, 9H), 1.5–1.9 (m, 3H), 4.3 (b-s, 1H), 5.1 (b-s, 1H), 7.3 (m, 1H), 7.8 (m, 2H), 8.3 (m, 2H), 8.5 (d, 1H), 8.6 (m, 1H), 8.9 (b-s, 1H). Found: C, 65.60; H, 7.34; N, 14.57%. Calcd for C₂₁H₂₈N₄O₃: C, 65.07; H, 7.42; N, 13.86%.

2.3. 4-(Boc-Pro-NH)-bpy

4-(Boc-Pro-NH)-bpy was prepared by the same method for 4-(Boc-Leu-NH)-bpy. $^1\text{H-NMR}$ (CDCl_3) δ = 1.51, 1.60 (ss, 9H), 1.98–2.51 (m, 4H), 3.48 (m, 2H), 4.48 (m, 1H), 7.30 (m, 1H), 7.79 (m, 4H), 8.38 (m, 2H), 8.58 (d, 2H), 8.69 (m, 1H). Found: C, 65.14; H, 6.49; N, 15.12%. Calcd for $\text{C}_{20}\text{H}_{24}\text{N}_4\text{O}_3$: C, 65.20; H, 6.57; N, 15.21%.

2.4. 4''-[N-[bis(4,4'-bis-trifluoromethyl-2,2'-bipyridine)(4'-methyl-2,2'-bipyridine-4-carbonyl)ruthenium(II)-Leu-NH]-bpy dichloride

A suspension of 4-(HCl·Leu-NH)-bpy (75 mg, 0.23 mmol) and N-methylmorpholine (0.026 ml, 0.23 mmol) in dry DMF (2 ml), a solution of 1-hydroxybenzotriazole (31 mg, 0.23 mmol) in DMF (1 ml), and EDC (0.050 ml, 0.27 mmol) were added successively to a stirred solution of $(\text{BTFMB})_2\text{Ru(II)}[4\text{-Me-bpy}(4'\text{-COOH})]\text{Cl}_2$ (168 mg, 0.23 mmol) in DMF (2.0 ml) at -20°C . The reaction mixture was stirred overnight at room temperature. After DMF was removed by rotary evaporation with a vacuum pump, the residue was chromatographed on a column of Sephadex LH-20 eluted with methanol to afford 4''-[$(\text{Ru(II)})(\text{BTFMB})_2\text{mb-4-CO-Leu-NH-bpy}$]. Treatment with aqueous ammonium hexafluorophosphate afforded PF_6 salt as a precipitate (**III**). $^1\text{H-NMR}$ (CD_3OD) δ = 0.9–1.1 (m, 6H), 1.7–2.0 (m, 3H), 2.6 (s, 3H), 1.98–2.51 (m, 4H), 7.4–9.4 (m, 25H), Found: C, 41.19; H, 2.87; N, 9.00%. Calcd for $\text{C}_{52}\text{H}_{40}\text{F}_{24}\text{N}_{10}\text{O}_2\text{P}_2\text{Ru}\cdot 3.3\text{H}_2\text{O}$: C, 41.22; H, 3.10; N, 9.24%.

2.5. 4''-[$(\text{Ru(II)})(\text{BTFMB})_2\text{mb-4-CO-Leu-NH-bpyOs(II)b}_2(\text{PF}_6)_4$, **I**(L = BTFMB) and other binuclear systems **I**(L = b), **II**(L = b and BTFMB)

A mixture of 4''-[$(\text{Ru(II)})(\text{BTFMB})_2\text{mb-4-CO-Leu-NH-bpy}$] (50.1 mg, 0.040 mmol) and $\text{Os(bpy)}_2\text{Br}_2$ (= $\text{Os(bpy)}_2\text{Br}_2$) (36.9 mg, 0.052 mmol) was refluxed in ethanol (40 ml) for 72 h under argon. The solid remaining after rotary evaporation was dissolved in methanol and chromatographed on a column of Sephadex LH-20 eluted with methanol to afford 4''-[$(\text{Ru(II)b}_2\text{mb-4-CO-Leu-NH-bpyOs(II)b}_2$)-(Cl₂Br₂) (52.3 mg, 65% yield). Treatment of the halide with ammonium hexafluorophosphate in water gave a PF_6 salt as a precipitate. $^1\text{H-NMR}$ (D_2O) δ = 0.9–1.0 (m, 6H), 1.6–2.0 (m, 3H), 2.6 (s, 3H), 7.2–8.8 (m, 41H). Boc-Leu- $\text{Os(II)b}_2(\text{PF}_6)_4$ (**IV**) was prepared from 4-(Boc-Pro-NH)-bpy and $\text{Os(bpy)}_2\text{Br}_2$ by the same procedure with **I**(L = BTFMB).

4''-[$(\text{Ru(II)b}_2\text{mb-4-CO-Leu-NH-bpyOs(II)b}_2(\text{PF}_6)_4$ **I**(L = b), 4''-[$(\text{Ru(II)b}_2\text{mb-4-CO-Pro-NH-bpyOs(II)b}_2(\text{PF}_6)_4$ **II**(L = b), and 4''-[$(\text{Ru(II)})(\text{BTFMB})_2\text{mb-4-CO-Pro-NH-bpyOs(II)b}_2(\text{PF}_6)_4$ **II**(L = BTFMB) were prepared by the same procedure with **I**(L = BTFMB). The purification was carried out by the chromatography on a column of Sephadex LH-20. The purity was evaluated by the NMR and luminescence measurements.

2.6. Physical measurements

Solvents for spectroscopic measurements were purchased from Nakarai Chemicals as in spectrograde. Static absorption and luminescence measurements were performed using a Shimadzu UV-2100 spectrometer and an RF-502A spectrofluorimeter, respectively. Room-temperature luminescence quantum yields, ϕ , were measured with $\text{Ru}(\text{bpy})_3^{2+}$ in deaerated water as a reference [10]. Samples for luminescence measurements were deoxygenated by purging with argon gas. The luminescence lifetime was measured by the time-correlated single photon counting method, as described elsewhere [11]. Electrochemical measurements were performed as described elsewhere [6].

3. Results and discussion

In Fig. 1 absorption spectra are presented for $(\text{BTFMB})_2\text{Ru}(\text{II})\text{mbCO-Leu-NHbpy-Os}(\text{II})\text{b}_2(\text{PF}_6)_4$ [**I** ($\text{L} = \text{BTFMB}$)] and its component complexes, $(\text{BTFMB})_2\text{-Ru}(\text{II})\text{mbCO-Leu-NHbpy}(\text{PF}_6)_2$ (**III**) and $\text{Boc-Leu-NHbpy-Os}(\text{II})\text{b}_2(\text{PF}_6)_4$ (**IV**) at the same substrate concentration. The spectrum of **I** ($\text{L} = \text{BTFMB}$) was identical with the superimposed spectrum of equimolar concentration of its component complexes, **III** and **IV**. For the bichromophoric system **I** and **II**, the electronic absorption spectrum can be described by a simple superposition of the absorption spectra of the two chromophores. The peptide-bridge serves as a molecular spacing unit which does not influence the basic electronic structure of the two chromophores while preventing intrachromophore interactions in the ground state. Compared with $\text{Ru}(\text{bpy})_3^{2+}$, lower energy-shift from 450 to 470 nm of metal-to-ligand and charge-transfer (MLCT) band was observed for **I** and **II** ($\text{L} = \text{BTFMB}$) systems and **III**, showing that BTFMB ligand has a lower lying π^* level. The lower energy shift of MLCT band was also observed for **I** and **II** ($\text{L} = \text{bpy}$) systems which contained the bpy-peptide ligand [bpy-CO-(Leu or Pro)].

I ($\text{L} = \text{BTFMB}$) shows two oxidation waves at ~ 1.5 and 0.74 V versus SCE for the $\text{Ru}(\text{III})/\text{Ru}(\text{II})$ and $\text{Os}(\text{III})/\text{Os}(\text{II})$ couples, and four reversible waves at -0.94 , -1.14 , -1.36 , and -1.51 V versus SCE for the ligand-based reduction for Ru

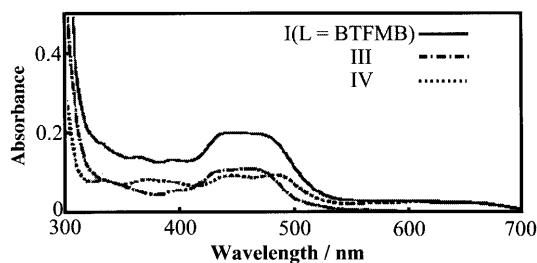


Fig. 1. Absorption spectra of **I** ($\text{L} = \text{BTFMB}$), **III** and **IV** in MeOH. [Substrate] = 2.2×10^{-5} M.

Table 1

Redox potentials for **I**(L = BTFMB and b), **III** and **IV**^{a,b}

Complex	$E_{1/2}$ /V vs. SCE					
	Ru(III/II)	Os(III/II)	(L ^{0/-1}) ₁	(L ^{0/-1}) ₂	(bpy ^{0/-1}) ₁	(bpy ^{0/-1}) ₂
I (L = BTFMB)	~ +1.5	+0.74	-0.94	-1.14	-1.36	-1.51
I (L = b)	+1.28	+0.79			~ -1.3	
III	+1.46		-0.94	-1.14		-1.87
IV		+0.79			-1.36	

^a Redox potentials [V vs. SCE, $E_{1/2} = (E_{pa} + E_{pc})/2$] were estimated from CV. Solvent, MeCN. Sweep rate, 100 mV/s⁻¹.

^b All complexes are PF₆ salts.

and Os components. These values correspond to those of **III** and **IV**, respectively. (Table 1). The sequence of reduction steps best interpreted as the stepwise reduction of each ligand π^* system. The strong σ -attracting CF₃ substituent is responsible for the shift of 0.4 V in first reduction of **I**(L = BTFMB) and **III**.

Room-temperature luminescence spectrum of **I**(L = BTFMB) (excitation wavelength: 455 nm) was recorded in argon-gas bubbled solutions and compared with those of **IV** and b₂Ru(II)mb-CO-Leu-NHbpyOs(II)b₂(PF₆)₄ **I**(L = bpy) at the same substrate concentration. As an illustration, the luminescence spectra of **I**(L = BTFMB), **IV**, and **I**(L = bpy) in MeOH are shown in Fig. 2. The efficient quenching of emission at 650 and 630 nm from the ruthenium complex was observed in **I**(L = BTFMB) and **I**(L = bpy), respectively. More than 98% of the potential luminescence of their ruthenium component (as measured for **III**) was

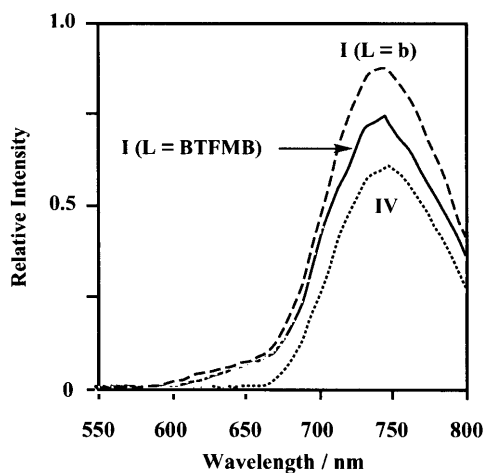


Fig. 2. Emission spectra (corrected) of **I**(L = b), **I**(L = BTFMB), and **IV** in MeOH. [Substrate] = 1.5×10^{-5} M. Excitation at 455 nm.

quenched in **I**(L = bpy and BTFMB). In the case of **I**(L = BTFMB), the enhancement of emission intensity of the osmium component at 750 nm was small in comparison with that of **I**(L = bpy). Lifetime measurements indicates that the intramolecular energy-transfer process in **I**(L = BTFMB) possessed a unitary efficiency. On the other hand, the sensitization of the osmium component was in about 50% efficiency (vide infra).

As for the quenching mechanism, energy transfer from $^*\text{Ru}(\text{II})$ to $\text{Os}(\text{II})$ and reductive electron transfer from $\text{Os}(\text{II})$ to $^*\text{Ru}(\text{II})$ are conceivable in the excited state of **I**(L = BTFMB). In acetonitrile, the first ligand-based reduction potential of $\text{BTFMB}^{0/-}$ couple and the first oxidation potential of the $\text{Os}^{3+/2+}$ couple of **I**(L = BTFMB) are -0.94 and 0.74 V versus SCE, respectively. The values of the excited-state energy (E_{0-0}) for **III** and **IV** based on the spectral fitting-method [12] were 1.94 and 1.69 eV, respectively. The photophysical behavior can be described in terms of an energy level diagram that is simply made by superimposing the low-lying excited states of the ruthenium and osmium units on the redox potentials in the ground state. Energy-transfer is also favorable by 0.25 eV in **I**(L = BTFMB) as well as **I**(L = bpy) ($\Delta G = -0.27$ eV). The reductive quenching of the excited Ru-complex is exergonic ($\Delta G = -0.20$ V) based on a reduction potential (0.94 V) for the $\text{Ru}^{2+*/+}$ couple with the oxidation potential (0.74 V) for the $\text{Os}^{3+/2+}$ couple. This is a remarkable feature of **I**(L = BTFMB), while the electron-transfer quenching process is endergonic in **I**(L = bpy). The thermodynamical aspect allows us to conclude that both energy transfer and electron transfer constitute the quenching mechanism in the excited state of **I**(L = BTFMB).

The measurement of luminescence lifetime was performed to evaluate the quenching on a quantitative basis by a time-correlated single-photon counting method. The decay of $\text{Ru}^{\text{II}} \rightarrow \pi^*(\text{BTFMB})$ MLCT emission at 630 nm and rise and decay of $\text{Os}^{\text{II}} \rightarrow \pi^*(\text{bpy})$ MLCT emission at 800 nm were measured in various solvents (excitation wavelength at 457.9 nm and instrumental width of 300 ps). Fig. 3 shows luminescence profiles of **I**(L = BTFMB) in MeOH at 293 K, with which a computer-calculated fit is superimposed. The luminescence profile can be fitted well by a convolution of a biexponential model $I_{\text{v}}(t) = A_1 \exp(-t/\tau_1) + A_2 \exp(-t/\tau_2)$ and the experimental instrument response function. Typical sets of parameter with amplitudes represented as percentages are presented in figures. At 630 nm the best fit was obtained with $\tau_1 = 6.5$ ns (98.4%) and $\tau_2 = 400$ ns (1.6%) (Fig. 3A). A minor, long-lived component can be attributed to a mononuclear ruthenium complex. The fast exponential decay (6.5 ns) is attributed to the deactivation of the ruthenium-excited state by the intramolecular quenching process. In Fig. 3B, the double exponential analysis for the rise and decay of the excited osmium complex at 800 nm gave $\tau_1 = 6.5$ ns and $\tau_2 = 36.5$ ns. The ratio of the preexponential factor of the double exponential function, namely A_2/A_1 was -2.4 . If the energy-transfer process has a unitary efficiency in this system, A_2/A_1 should be close to -1.9 . The deviation of A_2/A_1 from -1.9 indicates the existence of additional intramolecular quenching-process besides the energy-transfer process.

Kinetics of intramolecular processes in **I**(L = BTFMB) was evaluated by the following scheme. The excitation at 457.9 nm of **I**(L = BTFMB), denoted by

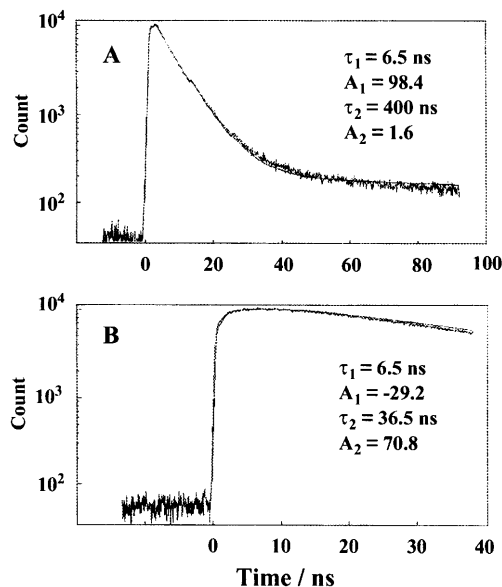


Fig. 3. Emission decay for **I**(L = BTFMB) in MeOH at 293 K. Monitored at 630 (A) and 800 (B) nm. Excitation at 457.9 nm. A computer calculated fit is superimposed.

Ru-Os, affords two excited states, namely *Ru-Os and Ru-Os* (Eq. (1a) and b). In addition to the normal deactivation process (Eq. (1c) and f), the additional quenching of *Ru-Os by an intramolecular electron-transfer process (Eq. (1d)) and the buildup of Ru-Os* by the intramolecular energy-transfer process (Eq. (1e)) are taken into account:



and



The relevant rate equations are

$$d[\text{*Ru-Os}]/dt = -(k_1 + k_{el} + k_{en})[\text{*Ru-Os}] \quad (2a)$$

and

$$d[\text{Ru-Os*}]/dt = k_{en}[\text{*Ru-Os}] - k_2[\text{Ru-Os*}] \quad (2b)$$

Eq. (2b) yields

$$[\text{Ru-Os}^*] = A_1 \exp[-(1/\tau_1)t] + A_2 \exp[-(1/\tau_2)t], \quad (3)$$

where $A_1 = k_{\text{en}}[*\text{Ru-Os}]_0/(1/\tau_2 - 1/\tau_1)$, $A_2 = [\text{Ru-Os}^*]_0 - A_1$, $1/\tau_1 = k_1 + k_{\text{el}} + k_{\text{en}}$, $1/\tau_2 = k_2$, and $[\text{*Ru-Os}]_0$ and $[\text{Ru-Os}^*]_0$ denote the initial concentration of *Ru-Os and Ru-Os^* , respectively. τ_1 can be obtained from the decay time at 630 nm and the rise time at 800 nm. τ_2 can be also obtained from the decay time at 800 nm. The values of k_2 calculated from τ_2 are in the range of $(2-5) \times 10^7 \text{ s}^{-1}$. The value of $k_1 \{(3-4) \times 10^6 \text{ s}^{-1}\}$ is based on the lifetime of its component complex **III** at room temperature. The ratio of molar absorption coefficients of its component complexes **IV** to **III** at 457.9 nm in MeOH was 0.9. The value of $[\text{Ru-Os}^*]_0/[*\text{Ru-Os}]_0 (= 0.9)$ was used for all solvents in this paper. The ratio of the preexponential factors of Eq. (3) is given by

$$A_2/A_1 = 0.9 \times (k_2 - k_1 - k_{\text{el}})/k_{\text{en}} - 1.9. \quad (4)$$

The rate constants k_{el} and k_{en} can be calculated from the observed set of values of A_2/A_1 , τ_1 , and τ_2 . The values of k_{el} and k_{en} in various solvents at room temperature are shown in Table 2. Both values are very close. As noted in the emission spectrum, the sensitization of the osmium component by the excited ruthenium component is in about 50% efficiency.

The mechanisms available for the transfer of electronic energy are based on remote dipole–dipole or dipole–multipole electronic interactions (the Förster mechanism) [13] and on a collisional mechanism that involves electronic exchange (the Dexter mechanism) [14,15]. A quantitative treatment of the Förster mechanism leads to the following expression for k_{en} : [13]

$$k_{\text{en}} = \frac{9000 \ln 10 \kappa^2 \phi_{\text{D}}}{128 \pi^5 n^4 N \tau_{\text{D}} R^6} \int_0^\infty \phi_{\text{D}}(n) \varepsilon_{\text{A}}(v) \frac{dv}{v^4} \quad (5)$$

Here, v is the wave number, $\phi_{\text{D}}(v)$ is the spectral distribution of the donor emission in quanta normalized to unity, $\varepsilon_{\text{A}}(v)$ is the molar extinction coefficient for the acceptor absorption, n is the refractive index of the solvent, κ is an orientation factor which equals $(2/3)^{1/2}$ for a random distribution of donor and acceptor molecules, ϕ_{D} is the quantum yield of donor emission, τ_{D} is the actual donor

Table 2
Rate constants of intramolecular energy and electron-transfer for **I**(L = BTFMB) and **II**(L = BTFMB)

Solvent	I (L = BTFMB) $\text{F}_2\text{Ru-Leu-Os}$		II (L = BTFMB) $\text{F}_2\text{Ru-Pro-Os}$	
	$k_{\text{en}}(\text{s}^{-1})$	$k_{\text{et}}(\text{s}^{-1})$	$k_{\text{en}}(\text{s}^{-1})$	$k_{\text{et}}(\text{s}^{-1})$
MeOH	8.6×10^7	6.5×10^7	7.7×10^7	4.6×10^7
EtOH	8.3×10^7	9.7×10^7	6.4×10^7	6.7×10^7
H ₂ O	1.4×10^8	8.4×10^7	1.2×10^8	4.0×10^7
CH ₃ CN	1.3×10^8	1.5×10^8	5.9×10^7	1.1×10^8
n-PrOH	9.3×10^7	8.7×10^7	6.6×10^7	7.5×10^7
n-BuOH	1.3×10^8	5.7×10^7	7.1×10^7	6.4×10^7

Table 3

Dipole–dipole distance R (nm) calculated from the Förster equation

Solvent	τ_0 /ns	ϕ_D	Overlap Int	I(L = BTFMB)		II(L = BTFMB)	
				$k_{\text{en}}(\text{obs})$	$R(\text{calc})$	$k_{\text{en}}(\text{obs})$	$R(\text{calc})$
MeOH	460	0.031	3.5×10^{-14}	$8.6 \times 10^7 \text{ s}^{-1}$	1.31	$7.7 \times 10^7 \text{ s}^{-1}$	1.33
EtOH	420	0.048	3.3×10^{-14}	8.3×10^7	1.41	6.4×10^7	1.47
H ₂ O	430	0.021	3.3×10^{-14}	1.4×10^8	1.13	1.2×10^8	1.16
CH ₃ CN	750	0.047	3.5×10^{-14}	1.3×10^8	1.21	5.9×10^7	1.30

emission lifetime, N is Avogadro's number, and R is the distance between the donor and acceptor molecules. The overlap integral was calculated from numerical integration over the emission of **III** and the absorption of **IV** in various solvents. The values are in the range of $(3.3\text{--}3.5) \times 10^{-14} \text{ mol}^{-1} \text{ cm}^6$. From Eq. (5), R values for **I** and **II** (L = BTFMB) were calculated and listed in Table 3. In Table 4, the distance of dipole–dipole for **I** and **II** (L = bpy), namely R was estimated with the observed rate constant and values of the corresponding model complexes.

It is known that the excited electron in MLCT excited state of $\text{Ru}(\text{bpy})_3^{2+}$ is fully localized on one of three equivalent ligands, at least for a time long enough for this ligand and its neighboring solvent to adjust to the geometry of fully charged bpy^- . Picosecond transient Raman studies on mixed-ligand derivatives of Ru(II) complexes have also shown that the optical electron is localized on the most easily reduced ligand [16]. In **I** and **II** (L = BTFMB), MLCT excitation takes place exclusively from ruthenium to bis(trifluoromethyl)bpy ligand (BTFMB). On the other hand, the lower lying π^* level is mb-CO bridging ligand in **I** and **II** (L = bpy).

Comparison of the dipole–dipole distances has been made in both systems with L = BTFMB and L = bpy in Tables 3 and 4. The intraligand distance in $\text{Ru}(\text{bpy})_3^{2+}$ is estimated to be about 0.5 nm from the molecular structure [17]. We assumed that the difference between the dipole–dipole distance is about 0.5 nm. From Table 3 and 4, the differences of R values in EtOH, H₂O, and CH₃CN are 0.48, 0.30, and 0.40 nm in **I** and 0.51, 0.31, and 0.47 nm in **II**, respectively. On average, these values are close to 0.5 nm. Therefore it is reasonable to conclude that the dipole–dipole interaction, namely the Förster mechanism, is the main pathway for intramolecular energy transfer in the excited **I** and **II** (L = BTFMB and bpy).

Table 4

Dipole–dipole distance R (nm) calculated from the Förster equation

Solvent	τ_0 /ns	ϕ_D	Overlap Int	I(L = bpy)		II(L = bpy)	
				$k_{\text{en}}(\text{obs})$	$R(\text{calc})$	$k_{\text{en}}(\text{obs})$	$R(\text{calc})$
EtOH	1120	0.034	5.1×10^{-14}	$6.7 \times 10^8 \text{ s}^{-1}$	0.93	$5.5 \times 10^8 \text{ s}^{-1}$	0.96
H ₂ O	425	0.012	3.8×10^{-14}	6.2×10^8	0.83	5.5×10^8	0.85
CH ₃ CN	1075	0.024	3.5×10^{-14}	7.4×10^8	0.81	6.2×10^8	0.83

The polypyridine Ru(II)/Os(II) binuclear system can be useful for the test of the mediation of peptide linkage in energy- and electron-transfer pocesses and especially useful as the probe for the determination of distance between two complexes in the polypeptide system.

References

- [1] K. Kalyanasundaram, *Photochemistry of Polypyridine and Porphyrin Complexes*, Academic Press, New York, 1992.
- [2] M. Furue, K. Maruyama, T. Oguni, M. Naiki, M. Kamachi, *Inorg. Chem.* 31 (1992) 3792.
- [3] M. Furue, K. Maruyama, Y. Kanematsu, T. Kushida, M. Kamachi, *Coord. Chem. Rev.* 132 (1994) 201.
- [4] B.P. Sullivan, D.J. Salmon, T.J. Meyer, *Inorg. Chem.* 17 (1978) 3334.
- [5] D.A. Buckingham, F.P. Dwyer, H.A. Goodwin, A.M. Sargeson, A. M. Aust. J. Chem. 17 (1964) 325.
- [6] M. Furue, T. Yoshidzumi, S. Kinoshita, T. Kushida, S. Nozakura, M. Kamachi, *Bull. Chem. Soc. Jpn.* 64 (1991) 1632.
- [7] A.B. Pepperman, *J. Org. Chem.* 46 (1981) (1981) 5039–5041.
- [8] D. Wenkert, R.B. Woodward, *J. Org. Chem.* 48 (1983) 283.
- [9] R.A. Jones, B.D. Roney, W.H.F. Sasse, K.O. Wade, *J Chem Soc (B)*, (1967) 106.
- [10] J. Van Houten, R.J. Watts, *J. Am. Chem. Soc.* 98 (1976) 4853.
- [11] S. Kinoshita, T. Kushida, *Anal. Instrum.* 14 (1985) 503.
- [12] E.M. Kober, J.V. Caspar, R.S. Lumpkin, T.J. Meyer, *J. Phys. Chem.* 90 (1986) 3722.
- [13] T. Förster, *Discussion Faraday Soc.* 27 (1959) 7.
- [14] D.L. Dexter, *J. Chem. Phys.* 21 (1953) 836.
- [15] B. Schlicke, P. Belser, L De Cola, E. Sabbioni, V. Balzani, *J. Am. Chem. Soc.* 121 (1999) 4207.
- [16] Y.J. Chang, X. Xu, T. Yabe, S.-C. Yu, D.R. Anderson, L.K. Orman, J.B. Hopkins, *J. Phys. Chem.* 94 (1990) 729.
- [17] M. Biner, H.-B. Bürgi, A. Ludi, C. Röhr, *J. Am. Chem. Soc.* 114 (1992) 5197.